AD-A043 804 SYRACUSE UNIV N Y DEPT OF ELECTRICAL AND COMPUTER E--ETC F/G 9/5
PATTERN MAGNITUDE SYNTHESIS FOR A REACTIVELY LOADED CIRCULAR AN--ETC(U)
AUG 77 J LUZWICK, R F HARRINGTON N00014-76-C-0225

UNCLASSIFIED TR-77-6 NL

1 OF 1
AD A043804

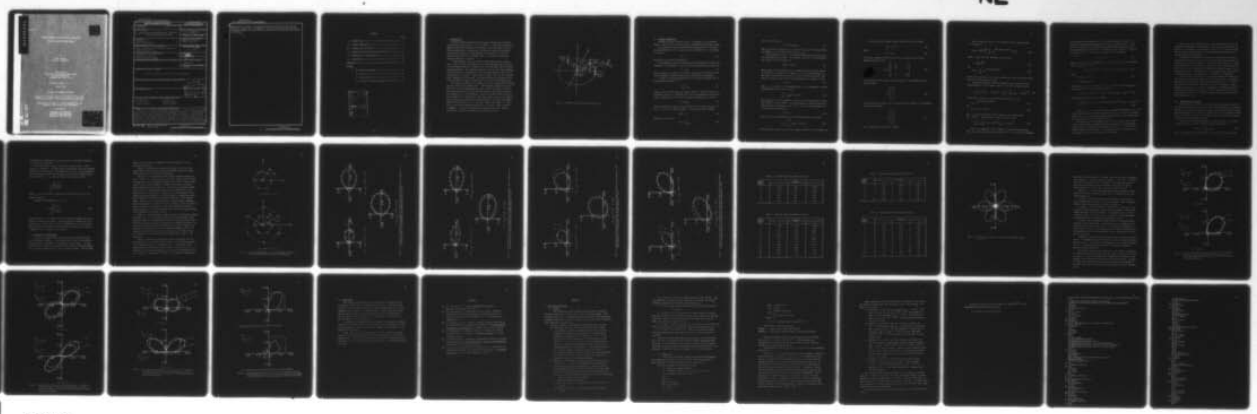

END
DATE FILMED
9-77
DDC

TR-77-6

(12)

PATTERN MAGNITUDE SYNTHESIS FOR A REACTIVELY LOADED CIRCULAR ANTENNA ARRAY

by

John Luzwick
Roger F. Harrington

Department of
Electrical and Computer Engineering
Syracuse University
Syracuse, New York 13210

Technical Report No. 6

August 1977

Contract No. N00014-76-C-0225

Prepared for

DEPARTMENT OF THE NAVY
OFFICE OF NAVAL RESEARCH
ARLINGTON, VIRGINIA 22217

UNCLASSIFIED

SECURITY CLASSIFICATION OF THIS PAGE *(When Data Entered)*

REPORT DOCUMENTATION PAGE

READ INSTRUCTIONS BEFORE COMPLETING FORM

1. REPORT NUMBER: TR-77-6	2. GOVT ACCESSION NO.
3. RECIPIENT'S CATALOG NUMBER	
4. TITLE *(and Subtitle)*: PATTERN MAGNITUDE SYNTHESIS FOR A REACTIVELY LOADED CIRCULAR ANTENNA ARRAY	5. TYPE OF REPORT & PERIOD COVERED: Technical Report No. 6
	6. PERFORMING ORG. REPORT NUMBER
7. AUTHOR(s): John Luzwick, Roger F. Harrington	8. CONTRACT OR GRANT NUMBER(s): N00014-76-C-0225
9. PERFORMING ORGANIZATION NAME AND ADDRESS: Dept. of Electrical and Computer Engineering, Syracuse University, Syracuse, New York 13210	10. PROGRAM ELEMENT, PROJECT, TASK AREA & WORK UNIT NUMBERS: 12 4pp.
11. CONTROLLING OFFICE NAME AND ADDRESS: Department of the Navy, Office of Naval Research, Arlington, Virginia 22217	12. REPORT DATE: Aug[redacted]977
	13. NUMBER OF PAGES: 40
14. MONITORING AGENCY NAME & ADDRESS *(if different from Controlling Office)*	15. SECURITY CLASS. *(of this report)*: UNCLASSIFIED
	15a. DECLASSIFICATION/DOWNGRADING SCHEDULE

16. DISTRIBUTION STATEMENT *(of this Report)*

Approved for public release; distribution unlimited

17. DISTRIBUTION STATEMENT *(of the abstract entered in Block 20, if different from Report)*

18. SUPPLEMENTARY NOTES

19. KEY WORDS *(Continue on reverse side if necessary and identify by block number)*

Antenna array
Circular array
Loaded antennas
Optimization
Pattern synthesis
Reactive loads

20. ABSTRACT *(Continue on reverse side if necessary and identify by block number)*

This report presents a method for synthesizing a given radiation field magnitude pattern for a reactively loaded circular dipole array. The reactively loaded circular dipole array has the center dipole fed and the outer dipoles parasitically excited with reactive loads across their input terminals. Both seven and thirteen element arrays are considered. A Rosenbrock optimization algorithm is applied directly to the synthesis error function to determine the reactive loads required for minimum error. Any arbitrarily shaped magnitude →

DD FORM 1 JAN 73 1473 EDITION OF 1 NOV 65 IS OBSOLETE
S/N 0102-014-6601

UNCLASSIFIED

SECURITY CLASSIFICATION OF THIS PAGE *(When Data Entered)*

406 737

pattern can be treated. The pattern magnitude synthesis results for the reactively loaded array are compared to that of an optimally excited array. A computer program for the optimization algorithm with operating instructions is included.

CONTENTS

		Page
I.	INTRODUCTION	1
II.	GENERAL FORMULATION	3
III.	OPTIMALLY EXCITED ARRAY	8
IV.	NORMALIZED SYNTHESIS ERROR AND Q-FACTOR	10
V.	REPRESENTATIVE COMPUTATIONS	11
VI.	CONCLUSIONS	28
REFERENCES		29
APPENDIX		
A.	The Subroutine ROSIEM	30
1)	Theory	30
2)	Description	31
3)	Listing of Subroutine ROSIEM	34

I. INTRODUCTION

Pattern synthesis methods exist for many different antenna arrays under various constraints [1]. In this report a radiation field pattern magnitude synthesis procedure for an N-port reactively loaded circular dipole antenna array is presented. The procedure applies an optimization algorithm directly to the synthesis error function to find the reactive loads required for minimum error. It accepts any arbitrary magnitude pattern as an input.

In many physical cases only the far field power pattern is specified. This, in effect, specifies the far field magnitude and leaves the far field phase arbitrary. Normally, the far field phase does not affect system performance. The synthesis procedure used in this report requires a specification of the magnitude of the far field electric field with no restrictions on the phase. Since the far electric field for the circular array considered in this report is linearly polarized, the square of the far field electric field is proportional to the far field power pattern.

The radiation pattern of an antenna array can be controlled by placing reactive loads at the antenna ports. The reactively loaded circular dipole array to be considered has the center dipole fed directly and the outer dipoles parasitically excited with reactive loads across their input terminals [2]. The advantage of reactively loaded antenna arrays is the elimination of a transmission line feed system to all of the elements. The circular array geometry was chosen because of its N-fold rotational symmetry with respect to ϕ in a constant θ plane (see Figure 1). Therefore, an arbitrary synthesized pattern in a constant θ plane is easier to realize. A reactively loaded linear array has much less symmetry which makes it harder to synthesize an arbitrary pattern.

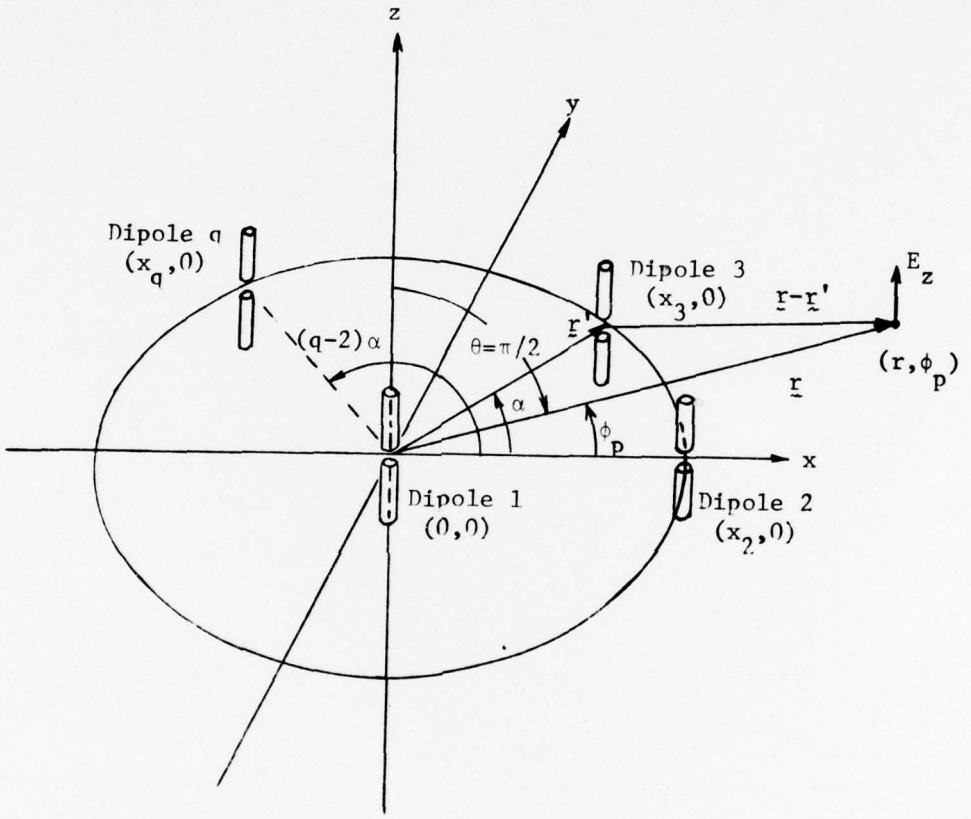

Fig. 1. Geometry of the circular antenna array.

II. GENERAL FORMULATION

Consider a source i and the field f it produces on the radiation sphere. Also, let T be a known operator representing the antenna system.

The analysis problem is concerned with determination of the radiation characteristics f for a given current distribution i of an antenna T, that is,

$$Ti = f \tag{1}$$

where this is an exact relationship.

The synthesis problem is concerned with determining the current distribution i of an antenna T given a specified field pattern f_o, that is,

$$Ti \approx f_o. \tag{2}$$

This is usually an inexact relationship. Deschamps and Cabayan [3] discuss the general inverse problem and the difficulties encountered.

In order to use matrix operations in the synthesis problem, (2) is discretized as follows. Let

$$i = \sum_{n=1}^{N} i_n e_n \tag{3}$$

where i_n are constants and e_n are basis elements. Since the source is continuous, the e_n are functions and (3) is an approximation to the true source. Define $\vec{i}$ to be the vector having the components i_n, that is,

$$\vec{i} = [i_n]_{N\times 1}. \tag{4}$$

Next, substitute (3) into (2) and evaluate (2) at P points (θ_p,ϕ_p), p = 1, 2, ..., P on the radiation sphere. In matrix notation, we have

$$[T]\vec{i} \approx \vec{f}_o \tag{5}$$

where $\vec{f}_o$ is the vector

$$\vec{f}_o = [f_{op}]_{P\times 1} \tag{6}$$

and [T] is the matrix

$$[T] = [(Te_n)_p]_{P\times N} \cdot \tag{7}$$

Here f_{op} denotes the value of $\vec{f}_o$ at the point (θ_p,ϕ_p) and $(Te_n)_p$ denotes the pattern of e_n evaluated at the point (θ_p,ϕ_p).

Next consider an array of N z-directed center-driven parallel one-half wavelength long dipoles. The boundary condition to be satisfied on the surface of the mth dipole is

$$-E_m(z) = V_m\delta(z) \tag{8}$$

where $E_m(z)$ is the z component of the tangential electric field induced by the electric currents on the dipoles, V_m is the voltage applied at the center of the mth wire, and $\delta(z)$ is the Dirac delta function. The electric current on the nth wire is approximated by a filament current

$$I_n \cos kz \tag{9}$$

where I_n is a constant to be determined and k is the propagation constant. Substituting (9) into (8), we obtain

$$-\sum_{n=1}^{N} I_n E_{mn}(z) = V_m\delta(z) \tag{10}$$

where $I_n E_{mn}(z)$ is the z component of the electric field induced by (9) on the surface of the mth dipole. Following Galerkin's method, we multiply (10) by cos kz and integrate from $-\lambda/4$ to $\lambda/4$ (λ is the wavelength) on z to obtain the matrix equation

$$[Z]\vec{I} = \vec{V}. \tag{11}$$

Here [Z] is the impedance matrix of the antenna array with elements

$$Z_{mn} = -\int_{-\lambda/4}^{\lambda/4} E_{mn}(z) \cos kz\, dz \tag{12}$$

and $\vec{I}$ and $\vec{V}$ are column vectors of the unknown currents I_n and voltages V_m.

For the reactively loaded circular dipole array, (11) becomes

$$[Z_A + Z_L]\vec{I} = \vec{V} \tag{13}$$

where

$$[Z_A] = [Z] \tag{14}$$

is the port impedance matrix for the circular dipole array with the elements defined by (12),

$$[Z_L] = \begin{bmatrix} 0 & 0 & \cdots & 0 \\ 0 & jX_L^2 & \cdots & 0 \\ \vdots & \vdots & & \vdots \\ 0 & 0 & \cdots & jX_L^n \end{bmatrix} \tag{15}$$

is the reactive load diagonal matrix where $jX_L^1 = 0$ corresponding to the central dipole,

$$\vec{V} = \begin{bmatrix} V^a \\ 0 \\ \vdots \\ 0 \end{bmatrix} \tag{16}$$

is the excitation voltage vector with one non-zero element V^a corresponding to the central dipole,

$$\vec{I} = \begin{bmatrix} I_1 \\ I_2 \\ \vdots \\ I_n \end{bmatrix} \tag{17}$$

is a column vector of the port currents.

The far electric field for the N dipoles in the ϕ direction and $\theta = \pi/2$ plane is

$$E_z(\phi) = \frac{-j\eta}{2\pi} \frac{e^{-jkr}}{r} \sum_{n=1}^{N} I_n e^{jk(x_n \cos\phi + y_n \sin\phi)} = KF(\phi) \tag{18}$$

where η is the intrinsic impedance of free space,

$$K = \frac{-j\eta}{2\pi} \frac{e^{-jkr}}{r} \tag{19}$$

and

$$F(\phi) = \sum_{n=1}^{N} I_n e^{jk(x_n \cos\phi + y_n \sin\phi)} . \tag{20}$$

Since we are interested only in the pattern shape, the far electric field $E_z(\phi)$ can be represented by $F(\phi)$.

The pattern magnitude synthesis procedure uses P points from the desired pattern $|\vec{f}_o|$ and finds a source $\vec{I}$ such that the pattern error

$$\varepsilon = \sum_{p=1}^{P} w_p \left| |F(\phi_p)| - |f_o(\phi_p)| \right|^2 = \sum_{p=1}^{P} w_p \left| \left| \sum_{n=1}^{N} I_n T_{pn} \right| - |f_o(\phi_p)| \right|^2 \tag{21}$$

is minimized. Here w_p is a weighting coefficient ($w_p > 0$),

$$T_{pn} = e^{jk(x_n \cos\phi_p + y_n \sin\phi_p)} \tag{22}$$

and

$$I_n = \{[Z_A + Z_L]^{-1}\vec{V}\}_n . \tag{23}$$

The $\{\ \}_n$ in (23) indicates the nth element of the column matrix $[Z_A + Z_L]^{-1}\vec{V}$. Substituting (23) into (21), we obtain

$$\varepsilon = \sum_{p=1}^{P} w_p \left| \left| \sum_{n=1}^{N} \{[Z_A + Z_L]^{-1}\vec{V}\}_n T_{pn} \right| - |f_o(\phi_p)| \right|^2 . \tag{24}$$

There are N unknowns in (24), namely, N-1 unknown reactive loads $\{X_L^n\}$ and one unknown excitation coefficient V^a. If $[Z_L]$ could be separated

out from the inverse operator in (24), an exact expression could be obtained for determining the required loads $\{X_L^n\}$ for minimum error. Since this is not mathematically feasible, an approximation technique is used for determining the $\{X_L^n\}$ and then incrementing these values in a direction which minimizes (24). One possible approach is the following.

Let

$$Z_L = jX_L + z_L \tag{25}$$

where z_L is an incremental change in Z_L. Then $[Z_A + Z_L]^{-1}$ can be expanded using a Maclaurin series as

$$[Z_A + jX_L + z_L]^{-1} \simeq [I + A + A^2 + \ldots][Z_A + jX_L]^{-1} \tag{26}$$

where

$$A = -[Z_A + jX_L]^{-1}[z_L] \tag{27}$$

I = identity matrix.

Assuming $[z_L]$ are small and the A^2, A^3, ... terms in (26) are negligible in relation to $[I + A]$, we can write (26) as

$$[Z_A + jX_L + z_L]^{-1} \simeq [I - [Z_A + jX_L]^{-1}[z_L]][Z_A + jX_L]^{-1}. \tag{28}$$

Substituting (28) into (24), we obtain

$$\varepsilon = \sum_{p=1}^{P} w_p \left|\left| \sum_{n=1}^{N} \{[I - [Z_A + jX_L]^{-1}[z_L]][Z_A + jX_L]^{-1}\vec{V}^e\}_n T_{rn} \right| - |f_o(\phi_p)| \right|^2. \tag{29}$$

If the A^2, A^3, ... terms in (26) are not negligible compared to $[I + A]$, new $\{X_L^n\}$ must be chosen and small changes made in z_L to test for a minimum. (Note that since (29) contains absolute value operations, the minimum does not necessarily occur at a stationary point.)

The advantage of this technique lies in the fact that $[z_L]$ in (29) can be varied without performing an inverse operation. A disadvantage is the fact that the $\{X_L^n\}$ have to be chosen so that A^2, A^3, ... are sufficiently small for (28) to hold. Also lacking is a good strategy for incrementing the $\{X_L^n\}$ in the direction of a minimum.

Another method of minimizing (24) is the direct application of an optimization algorithm. This approach is used in this report since the method is not dependent on the proximity of the $\{X_L^n\}$ to a minimum point, and the optimum seeking strategy for incrementing the variables is an integral part of the algorithm.

The optimization subroutine selected is a Rosenbrock algorithm [4]. The Rosenbrock algorithm uses a set of N mutually orthogonal directions in each cycle of searches (stage). After each stage, a new set of orthogonal directions are determined by rotating the former direction vectors until they are oriented toward the direction of fastest decrease of the objective function. A description of the Rosenbrock algorithm along with a computer listing of the subroutine is included in the Appendix.

In this report N variables are used in the Rosenbrock subroutine -- N-1 reactive loads and one excitation voltage coefficient. It should be mentioned that since (24) does not depend on the phase of V^a, V^a can be taken as real and positive. When this is done, (24) becomes a simple quadratic function in V^a. From this quadratic, the optimum value of V^a can be easily obtained for fixed Z_L. If this optimum value of V^a were substituted back into (24), only the N-1 reactive loads would enter into the Rosenbrock search.

III. OPTIMALLY EXCITED ARRAY

In this section, a solution is given for the same array analyzed in the preceding section, but with all of the elements driven and no reactive loading. In the results section, a comparison of the synthesized patterns will be made between the reactively loaded array and the optimally excited array to indicate the degree of degradation due to the restricted excitation for the reactively loaded array.

The far electric field magnitude at a point p in the $\theta = \pi/2$ plane has the same form as in the reactively loaded case, that is,

$$|F(\phi_p)| = \left| \sum_{n=1}^{N} i_n T_{pn} \right|. \tag{30}$$

Here, i_n can take on any complex value, in contrast to the restricted

values for the reactively loaded case. A solution for the pattern magnitude synthesis problem using (30) can be found in [5], and the following is a summary of the formulation.

The error function to be minimized for the general synthesis problem where both magnitude and phase of the desired pattern $\vec{f}_o$ are specified is

$$\varepsilon = \sum_{p=1}^{P} w_p \left| \sum_{n=1}^{N} i_n T_{pn} - f_o(\phi_p) \right|^2. \tag{31}$$

The solution to (31) (see section V of [5] with $\alpha = 0$) is

$$\vec{i} = [\tilde{T}^* W T]^{-1} [\tilde{T}^* W] \vec{f}_o \tag{32}$$

where * signifies complex conjugate, $\tilde{}$ signifies transpose and [W] is a weighting matrix.

When the pattern magnitude only is specified, the error function becomes

$$\varepsilon = \sum_{p=1}^{P} w_p \left| \left| \sum_{n=1}^{N} i_n T_{pn} \right| - |f_o(\phi_p)| \right|^2. \tag{33}$$

To circumvent the inner magnitude operation in (33), we consider the following more general equation which has a minimum less than or equal to that of (33),

$$\varepsilon(\vec{\beta}) = \sum_{p=1}^{P} w_p \left| \sum_{n=1}^{N} i_n T_{pn} - |f_o(\phi_p)| e^{j\beta_p} \right|^2. \tag{34}$$

In other words, we are specifying a phase for the pattern magnitude in order to obtain a more easily solved expression. For i_n fixed, a minimum is obtained when both terms within the outer magnitude signs of (34) are in phase, that is,

$$e^{j\beta_p} = \frac{\sum_{n=1}^{N} i_n T_{pn}}{\left| \sum_{n=1}^{N} i_n T_{pn} \right|}. \tag{35}$$

If condition (35) is used in minimizing (34), the minimum of (34) will be equal to the minimum of (33). (This can be shown by substituting (35) into (34), and after factorization it is evident that the magnitude of the resulting expression will be equal to that of (33).)

To find the minimum of (34), the following iterative procedure is used:

1. Assume starting values for $\beta_1, \beta_2, \ldots, \beta_p$.
2. Keep the β_p fixed and calculate the i_n which minimizes ε using (32).[1]
3. Keep the i_n fixed and calculate the β_p which minimizes ε using (35).
4. Go to step (2).

This procedure converges to a stationary point because steps (2) and (3) cannot increase ε.

IV. NORMALIZED SYNTHESIS ERROR AND Q-FACTOR

Two figures of merit will be used in the next section to evaluate the synthesis results. The first figure of merit is the normalized synthesis error which is defined as

$$\varepsilon_{syn} = \frac{\sum_{p=1}^{P} w_p \left| |F(\phi_p)| - |f_o(\phi_p)| \right|^2}{\sum_{p=1}^{P} w_p |f_o(\phi_p)|^2} . \qquad (36)$$

[1] It should be noted that if $[\tilde{T}^*WT]$ is ill-conditioned, the procedure will fail since small rounding errors that occur in its inversion can cause large errors in its inverse $[\tilde{T}^*WT]^{-1}$. To use this procedure, the ratio of the magnitude of the largest eigenvalue to the smallest of $[\tilde{T}^*WT]$ should be on the order of 10^3 or less.

The smaller the magnitude of ε_{syn} the closer the synthesized pattern is to the desired pattern.

The second figure of merit is the Q or quality factor. The Q-factor is a measure of the magnitudes of the element excitation required to produce a given pattern. The larger the value of Q, the more impractical the pattern realization becomes due to the large element excitations required. Lo, Lee, and Lee defined the Q-factor as [6]:

$$Q = \frac{\sum_{n=1}^{N} |J_n|^2}{\int_{4\pi} |P(\theta,\phi)|^2 d\Omega} \tag{37}$$

where J_n is the nth element current excitation value and $P(\theta,\phi)$ is a pattern function.

A numerical approximation to (37) is

$$Q = P \frac{\sum_{n=1}^{N} |i_n|^2}{\sum_{p=1}^{P} |F(\phi_p)|^2} \tag{38}$$

The multiplier P is introduced to make Q relatively insensitive to the number of field points chosen. The main difference between the Q expressions of (37) and (38) is that the denominator of (37) is an integral over the whole radiation sphere while the denominator of (38) is a summation over P points in the XY plane.

V. REPRESENTATIVE COMPUTATIONS

A computer program has been written using the equations derived in the preceding sections. A description and listing of the optimization subroutine is included in the Appendix of this report. In this section results are given to illustrate the synthesis technique applied to a reactively loaded array for various pattern shapes. For all cases

except the reduction of an unwanted side lobe (Figure 13) all w_p used are equal to one.

Figure 2 illustrates the antenna configurations for both the seven element (array A) and the thirteen element (array B) circular arrays to be used in the synthesis procedure.

Figures 3 to 6 illustrate Gaussian shaped synthesis patterns in the $\phi = 0$ and $\phi = 30°$ directions for reactively loaded arrays A and B in which the specified pattern beam widths are varied. For all cases array B (with a greater number of elements than array A) realized lower synthesis errors than array A. The worst case (largest synthesis error) of the three pattern shapes to be synthesized for both arrays A and B is pattern (a). Pattern (a) is the narrowest of the three patterns and apparently a greater number of elements than thirteen is needed to realize the directivity required by this pattern shape. Pattern (b) is synthesized with a slightly higher synthesis error than pattern (c) for array A but the reverse is true for array B. Overall, pattern (b) appears to be the best compromise in terms of pattern synthesis error and distortion when specifying a pattern shape to be synthesized for arrays A and B.

Tables 1-4 list the reactive loads required for the patterns shown in Figures 3-6. Note that loads which affect the beam width in one direction (therefore changing their values for each beam width variation) do not necessarily affect the pattern in another direction. For instance, the reactive load for element four in Table 1 varies from +26 ohms to +90 ohms as the pattern beam width changes in the $\phi = 0$ direction while the reactive load for element four in Table 3 does not change at all as the pattern beam width changes in the $\phi = 30°$ direction.

Figure 5 illustrates an important property (necessary for synthesizing patterns in arbitrary directions) of the circular array due to its symmetry, that is, a pattern in the $\phi = 0$ direction can be shifted exactly (for arrays A and B) to the $\phi = n60°$, $n = 1, 2, \ldots, 5$ directions by cyclically changing the reactive loads required for the $\phi = 0$ direction. The pattern in Figure 7 is obtained by taking the

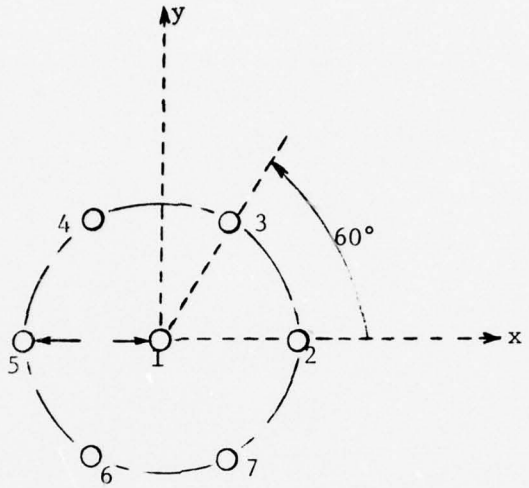

(a) Array A - N = 7

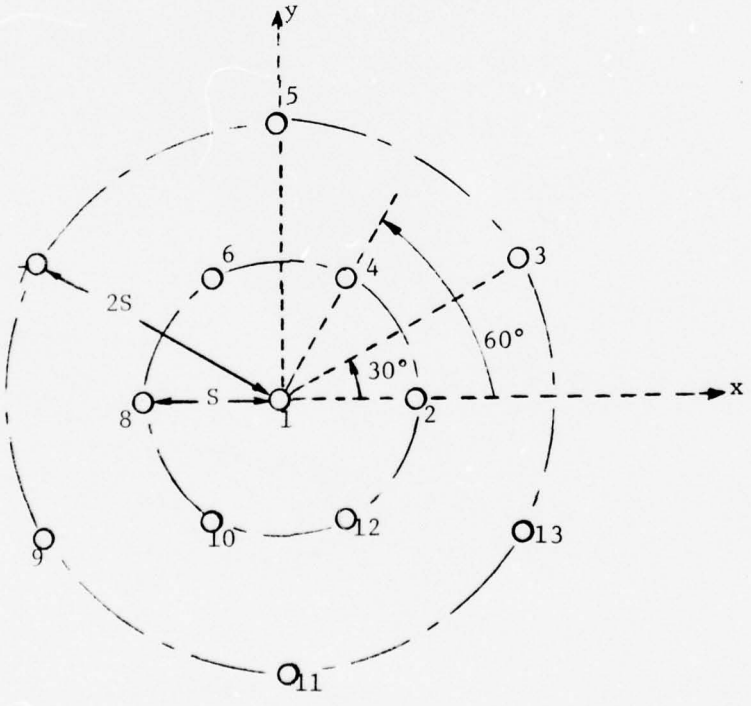

(b) Array B - N = 13

Fig. 2. Antenna configuration for a seven element (array A) and thirteen element (array B) circular array.

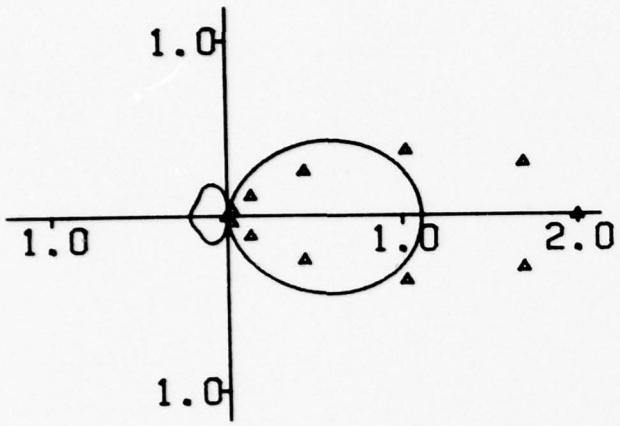

(a) $\varepsilon_{syn} = 0.28, \quad Q = 5.52$

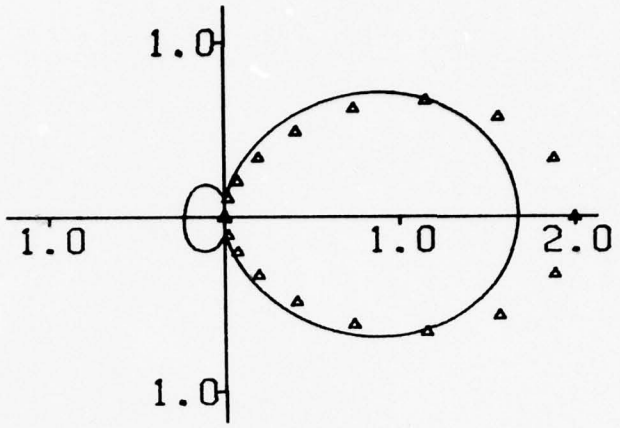

(b) $\varepsilon_{syn} = 0.06, \quad Q = 4.26$

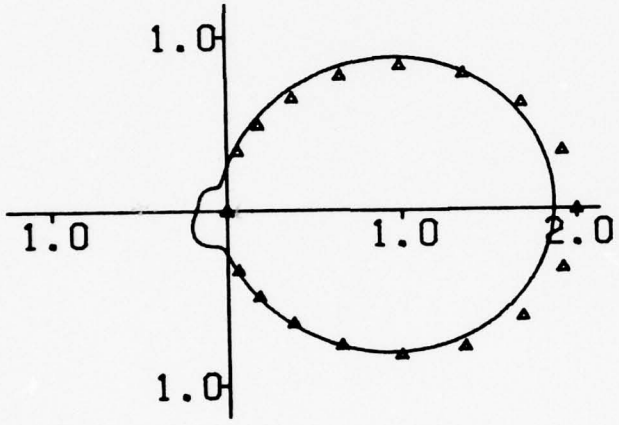

(c) $\varepsilon_{syn} = 0.03, \quad Q = 3.47$

Fig. 3. Far electric field pattern variations for reactively loaded circular array A where $\phi = 0$, Δ - pattern shape to be synthesized, and element spacing $s = 0.25\lambda$.

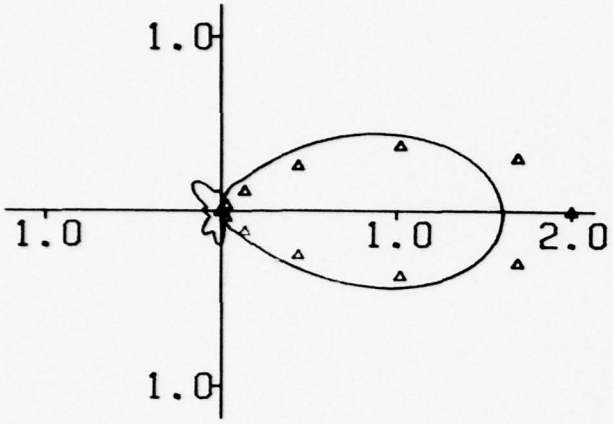

(a) $\varepsilon_{syn} = 0.10$, $Q = 22.04$

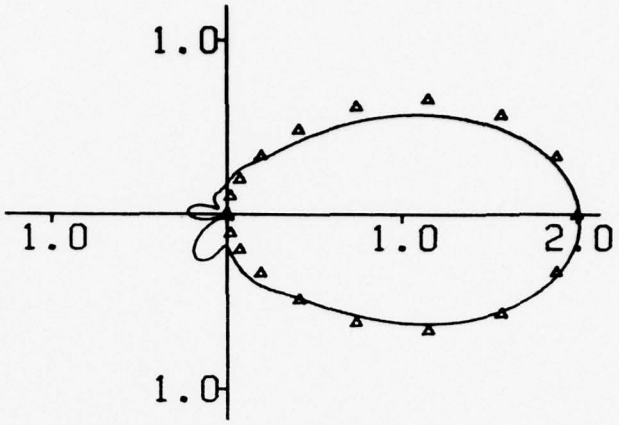

(b) $\varepsilon_{syn} = 0.04$, $Q = 10.29$

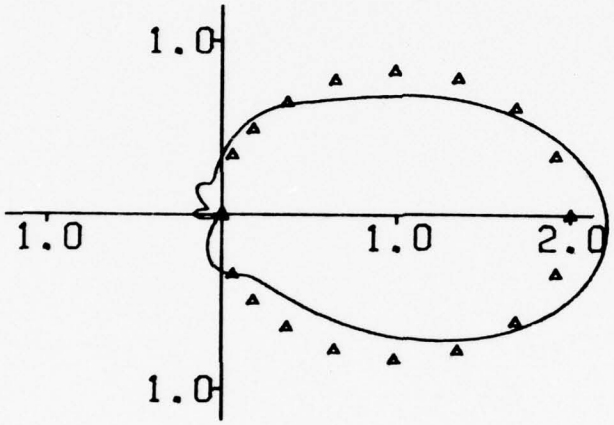

(c) $\varepsilon_{syn} = 0.05$, $Q = 3.91$

Fig. 4. Far electric field pattern variations for reactively loaded circular array B where $\phi = 0$, Δ-pattern shape to be synthesized, and element spacing $s = 0.25\lambda$.

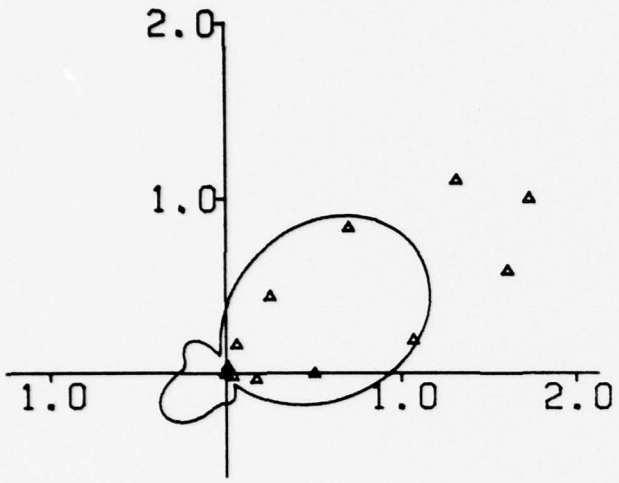

(a) $\varepsilon_{syn} = 0.34, \quad Q = 4.58$

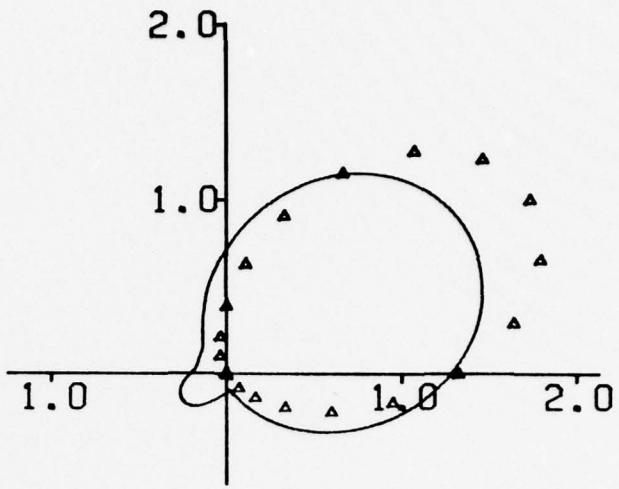

(b) $\varepsilon_{syn} = 0.08, \quad Q = 3.12$

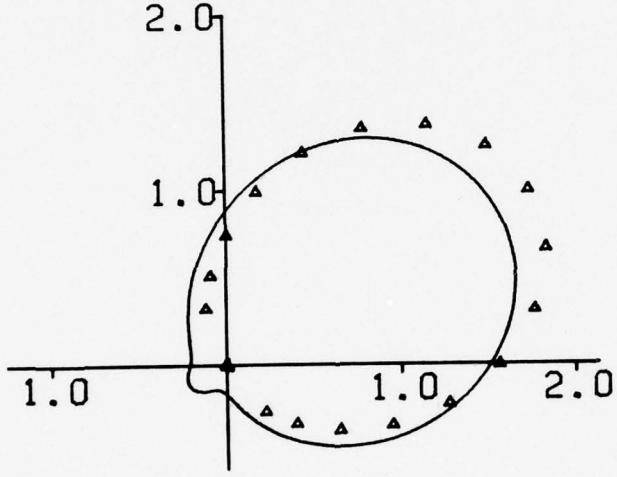

(c) $\varepsilon_{syn} = 0.05, \quad Q = 2.52$

Fig. 5. Far electric field pattern variations for reactively loaded circular array A where $\phi = 30°$, Δ-pattern shape to be synthesized, and element spacing $s = 0.25\lambda$.

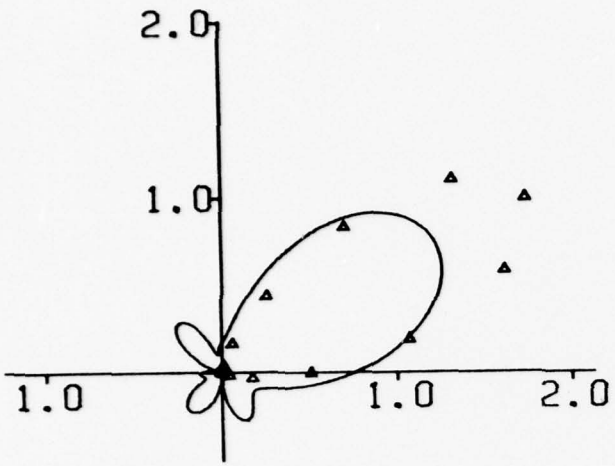

(a) $\varepsilon_{syn} = 0.18, \quad Q = 11.01$

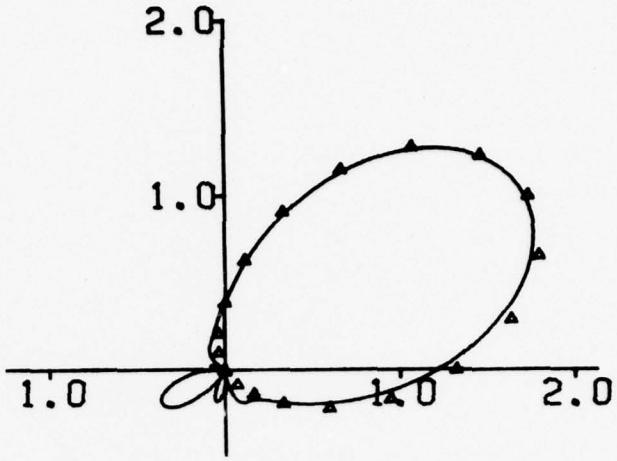

(b) $\varepsilon_{syn} = 0.03, \quad Q = 6.64$

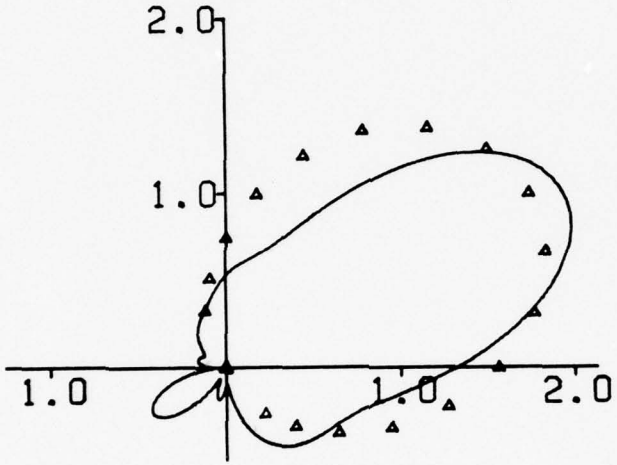

(c) $\varepsilon_{syn} = 0.09, \quad Q = 7.58$

Fig. 6. Far electric field pattern variations for reactively loaded circular array B where $\phi = 30°$, Δ-pattern shape to be synthesized, and element spacing $s = 0.25\lambda$.

Table 1. Reactive loads for patterns in Fig. 3.

Element Number	Pattern		
	1	2	3
2	- 73Ω	- 86Ω	-105Ω
3	-109	-107	-117
4	+ 26	+ 65	+ 90
5	+ 18	+ 11	+ 13
6	+ 23	+ 61	+ 90
7	-101	-111	-127

Table 2. Reactive loads for patterns in Fig. 4.

Element Number	Pattern		
	1	2	3
2	- 95Ω	- 99Ω	-103Ω
3	- 52	- 60	- 68
4	- 93	- 97	-103
5	+ 30	+ 26	+ 17
6	-249	+135	+ 17
7	- 27	- 20	+172
8	- 33	- 8	- 13
9	-118	+ 87	+111
10	-197	+291	- 4
11	+151	+ 74	+ 23
12	- 69	- 95	- 96
13	- 69	- 72	- 72

Table 3. Reactive loads for patterns in Fig. 5.

Element Number	Pattern		
	1	2	3
2	- 70Ω	-109Ω	-134Ω
3	+ 69	-115	-147
4	-300	-300	-300
5	+ 36	+ 36	+ 36
6	+ 15	+ 21	+ 34
7	-300	-300	-300

Table 4. Reactive loads for patterns in Fig. 6.

Element Number	Pattern		
	1	2	3
2	- 71Ω	- 67Ω	- 65Ω
3	-106	-202	-300
4	- 56	- 69	- 56
5	- 95	-101	-101
6	- 91	- 89	- 82
7	- 16	+ 10	+ 35
8	- 43	- 40	- 36
9	- 30	- 33	-300
10	- 32	- 33	- 26
11	- 6	+ 27	+ 15
12	- 97	-100	- 83
13	+ 53	- 94	- 93

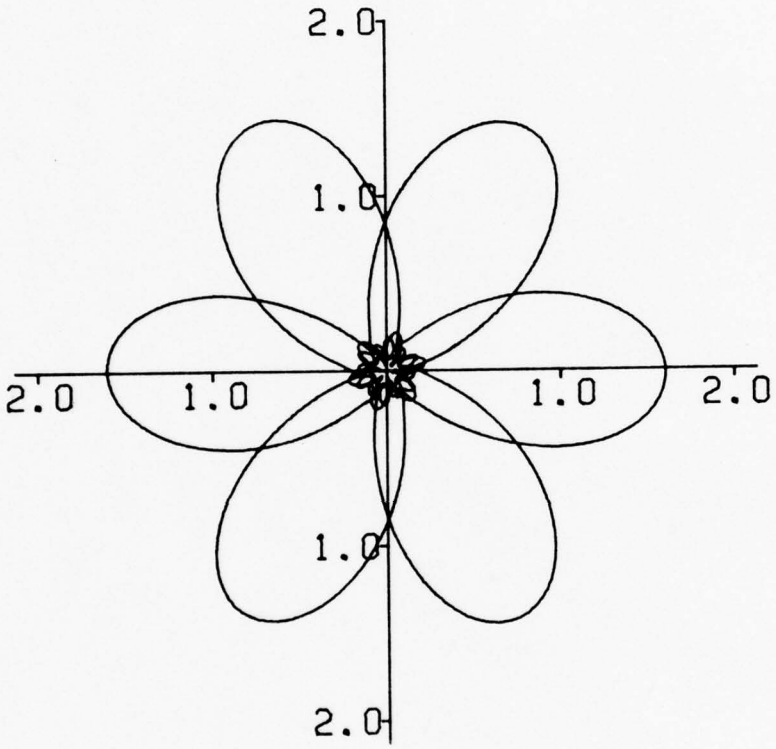

Fig. 7. Pattern superposition for array B with element spacing $s = 0.25\lambda$.

reactive loads for pattern 1 of Figure 4 and shifting them accordingly. For instance, to shift the pattern from the $\phi = 0$ to the $\phi = 60°$ direction, the reactive load value for element two becomes the reactive load value for element four; the reactive load value for element three becomes the reactive load value for element five, etc.

Figures 8 to 10 illustrate synthesized patterns having a single main lobe for both optimally excited (used for comparison) and reactively loaded arrays.

In Figure 8 a Gaussian shaped pattern similar in beam width to that of pattern (b)in Figures 3 to 6 is synthesized. Both excitations achieve a low synthesis error with about the same Q.

In Figure 9, a sector pattern is synthesized. Since this is not a natural pattern shape, each excitation type attempts to distort the normal beam shape to fit the contour. The synthesis error for both excitation types is still low due to the relatively large beam width required (realizable as illustrated in Figures 3 to 6).

In Figure 10, a rectangular shaped pattern is synthesized which requires a narrow beam width. The synthesis error is higher for this case than in the previous two cases. A linear array configuration would probably realize a lower synthesis error than the circular array configuration due to the increased directivity characteristics in the end fire direction.

An attempt to synthesize multiple main lobes is shown in Figures 11 and 12. The synthesized patterns obtained for array B are much better than for array A. This degree of improvement is not evident in Figures 8 to 10. It appears that more elements are needed to synthesize multiple shaped beam patterns.

The pattern illustrated in Figure 13b is an attempt to synthesize the sector shaped pattern without the side lobe indicated by the arrow in Figure 13a. This is accomplished by weighting the synthesis error greater in the arrow direction than in all other directions. As shown in Figure 13b, the unwanted side lobe is decreased at the expense of increased side lobes in other directions and greater overall synthesis error.

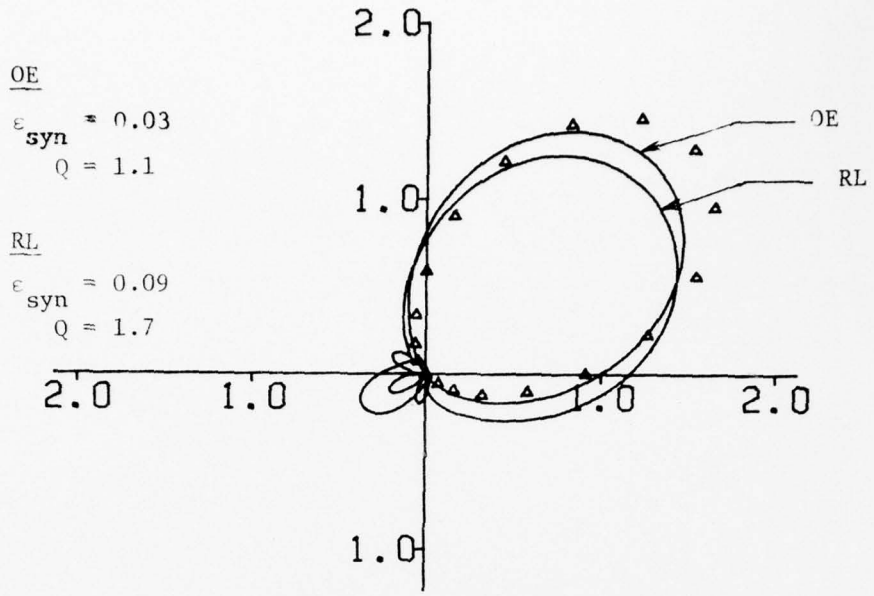

(a) Array A

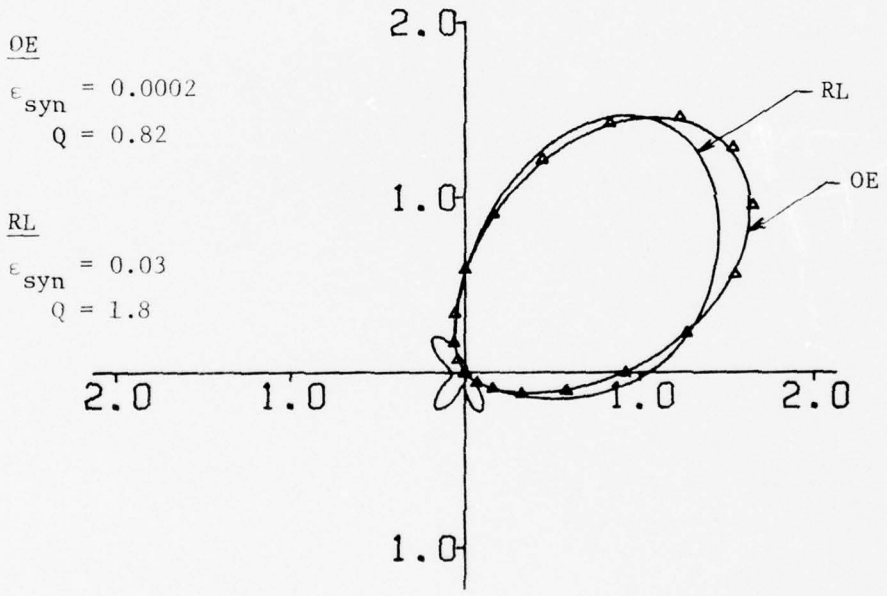

(b) Array B

Fig. 8. Far electric field synthesized patterns for a reactively loaded circular array with element spacing s = 0.35λ (Δ-pattern shape to be synthesized, OE-optimally excited, RL-reactive loading).

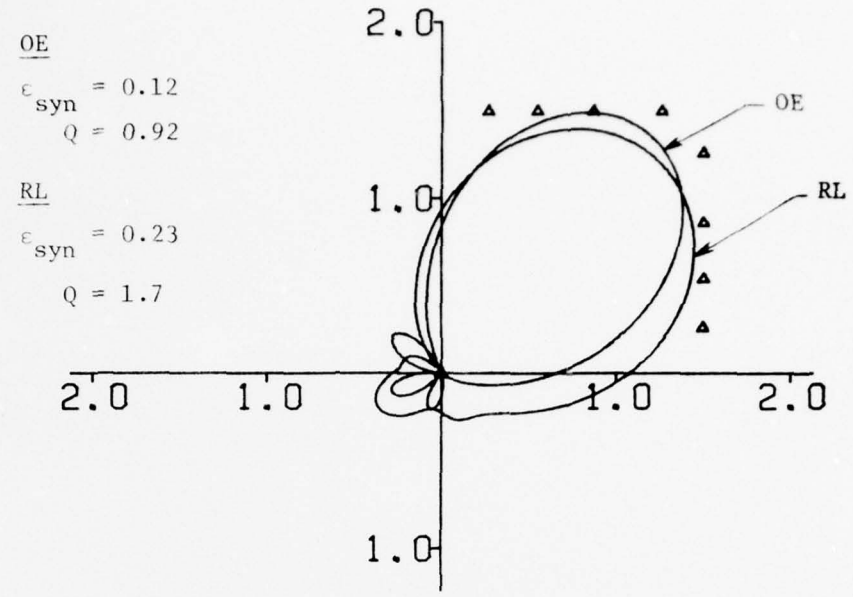

(a) Array A

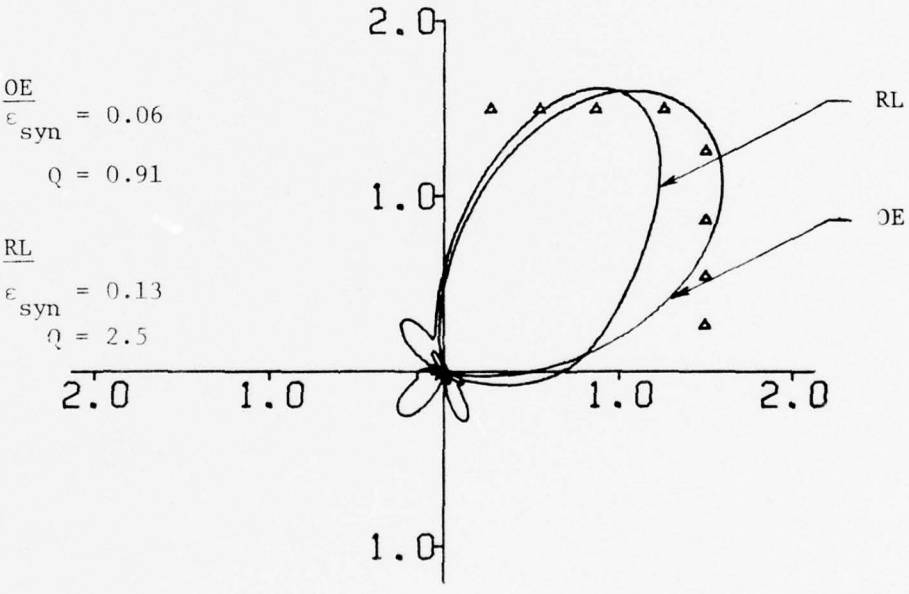

(b) Array B

Fig. 9. Far electric field synthesized patterns for a reactively loaded circular array with element spacing s = 0.35λ (Δ-pattern shape to be synthesized, OE-optimally excited, RL-reactive loading).

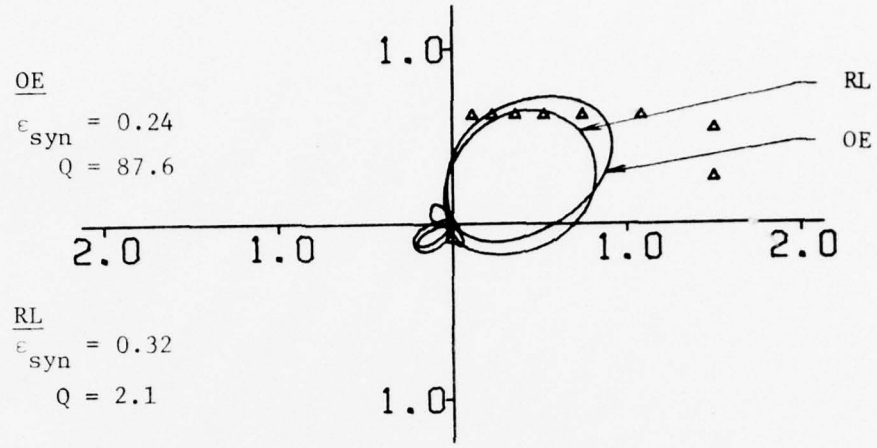

(a) Array A

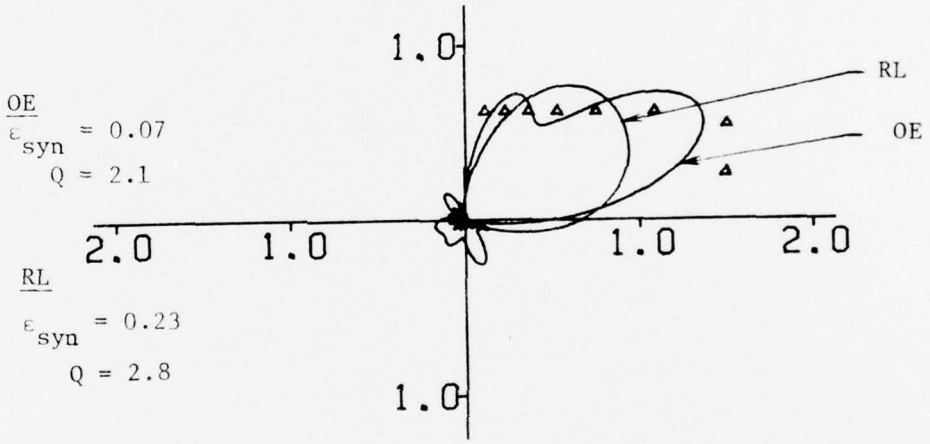

(b) Array B

Fig. 10. Far electric field synthesized patterns for a reactively loaded circular array with element spacing s = 0.35λ (Δ-pattern shape to be synthesized, OE-optimally excited, RL-reactive loading).

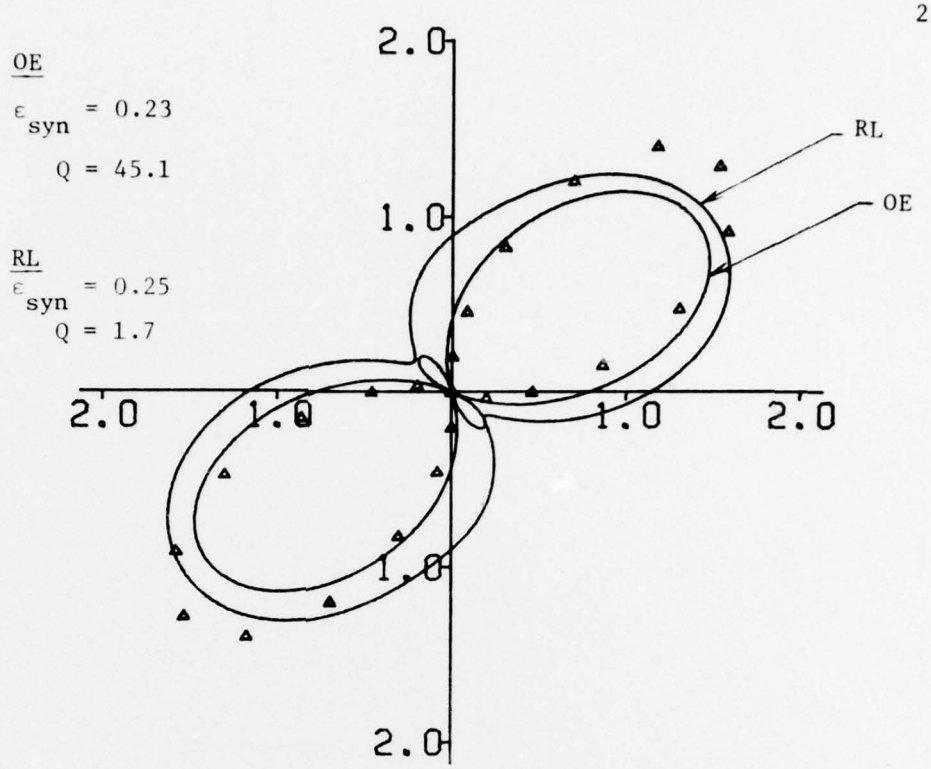

(a) Array A

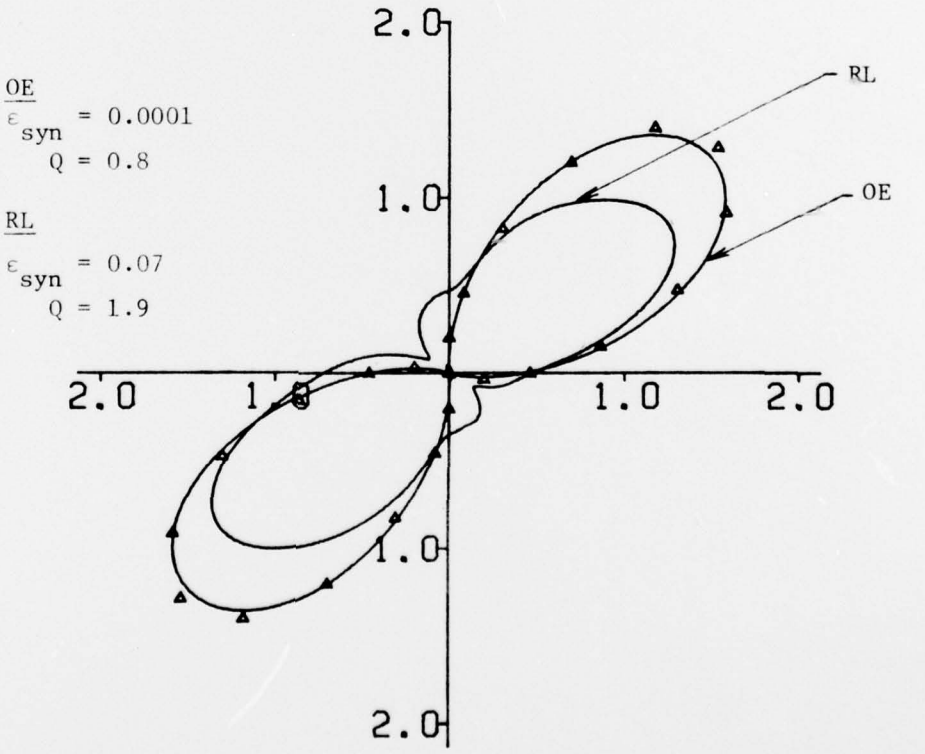

(b) Array B

Fig. 11. Far electric field synthesized patterns for a reactively loaded circular array with element spacing s = 0.35λ (Δ-pattern shape to be synthesized, OE-optimaliy excited, RL-reactive loading).

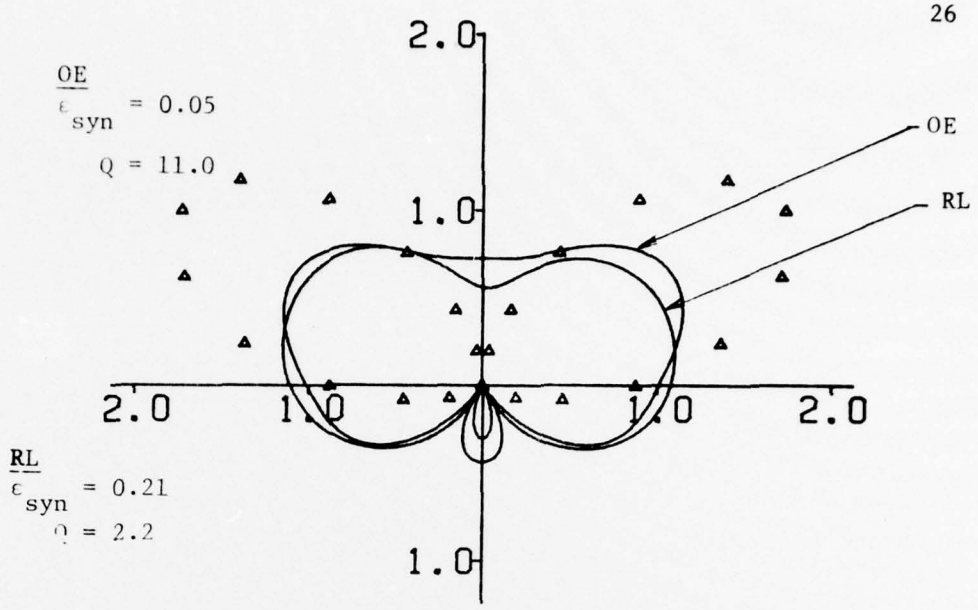

(a) Array A

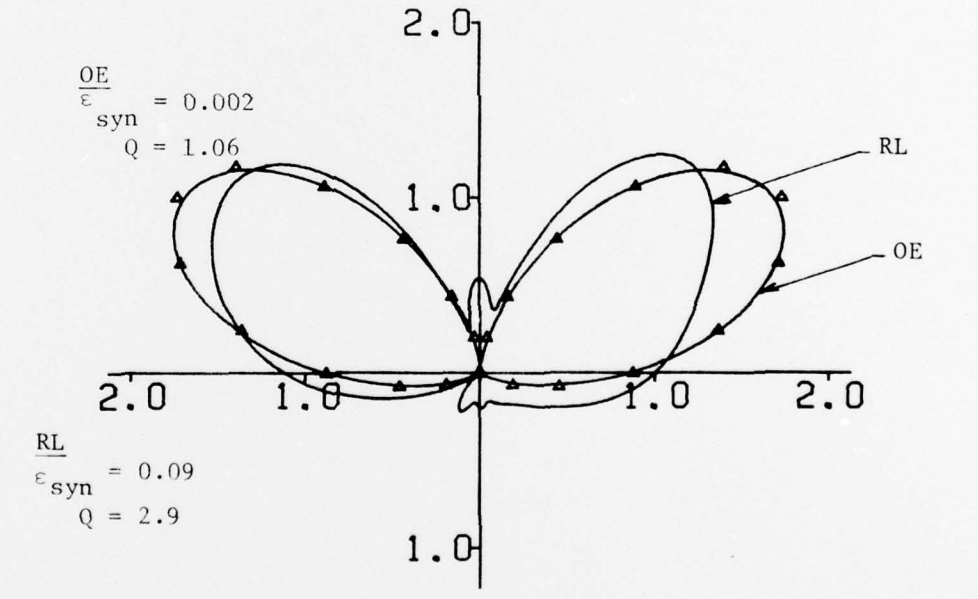

(b) Array B

Fig. 12. Far electric field synthesized patterns for a reactively loaded circular array with element spacing s = 0.35λ (Δ-pattern shape to be synthesized, OE-optimally excited, RL-reactive loading).

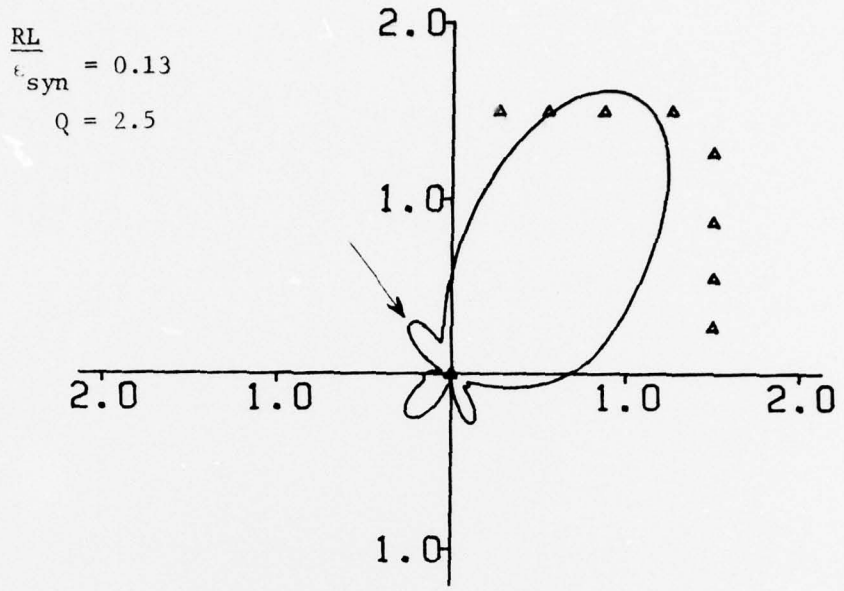

(a) Synthesized pattern with unwanted side lobe.

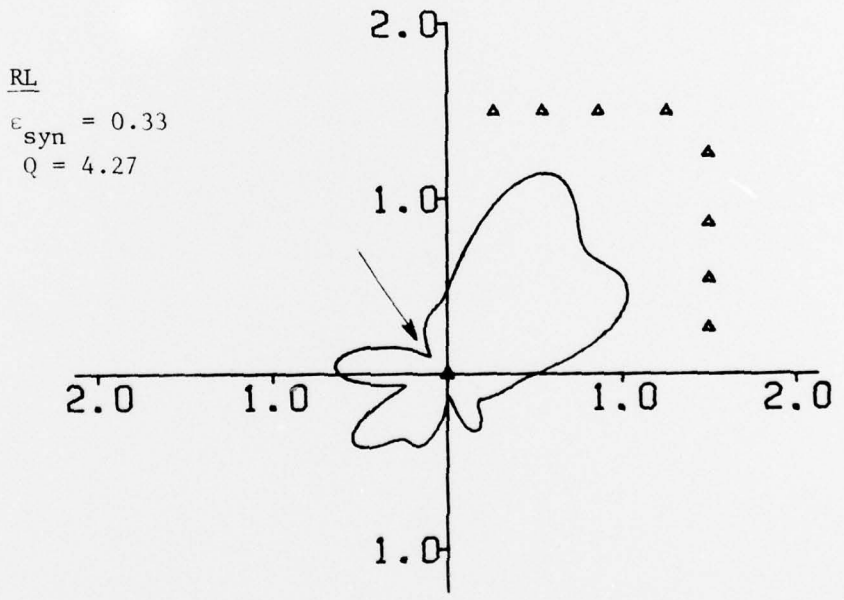

(b) Synthesized pattern with unwanted side lobe removed.

Fig. 13. Synthesized pattern with side lobe restriction for array B with element spacing s = 0.35λ (Δ-pattern shape to be synthesized, RL-reactive loading, ↘ -unwanted side lobe direction).

VI. CONCLUSIONS

The antenna element currents for the reactively loaded array are a subset of currents for the optimally excited array. Therefore, while the error in the reactively loaded array patterns approaches that of the optimally excited array, it is always greater. The patterns are closest when the specified shape is typical of the patterns realizable by reactively loaded arrays (pattern (b) in Figures 3-6). Verification of this statement is shown in Figure 8.

The synthesis technique used in this report is adaptable to problems involving more variables, like antenna element length and position. Also, various weighting functions can be used to improve the convergence of the optimization algorithm.

Future work should investigate more fully the correlation between antenna array configuration and synthesis pattern shapes for reactively loaded arrays. These results would allow specifying an antenna array configuration for a corresponding pattern shape before the synthesis procedure has begun.

REFERENCES

[1] R.E. Collin and F.J. Zucker, Antenna Theory - Part I. New York: McGraw-Hill, 1969, ch. 7.

[2] R.F. Harrington, R.F. Wallenberg, and A.R. Harvey, "Design of Reactively Controlled Antenna Arrays," Technical Report No. 4, Contract No. N00014-67-A-0378-0006, Office of Naval Research, September 1975.

[3] G.A. Deschamps and H.S. Cabayan, "Antenna Synthesis and Solution of Inverse Problems by Regularization Methods," IEEE Transactions on Antennas and Propagation, vol. AP-20, May 1972, pp. 268-274.

[4] H.H. Rosenbrock, "An Automatic Method for Finding the Greatest or Least Value of a Function," The Computer Journal, 3, October 1960, pp. 175-184.

[5] J.R. Mautz and R.F. Harrington, "Computational Methods for Antenna Pattern Synthesis," IEEE Transactions on Antennas and Propagation, vol. AP-23, July 1975, pp. 507-512.

[6] Y.T. Lo, S.W. Lee, and Q.H. Lee, "Optimization of Directivity and Signal-to-Noise Ratio of an Arbitrary Antenna Array," Proceedings of the IEEE, vol. 54, August 1966, pp. 1033-1045.

APPENDIX

A. THE SUBROUTINE ROSIEM

1) Theory:

The Rosenbrock search technique uses N mutually orthogonal directions during each search cycle to find a relative minimum. This strategy differs from a steepest descent technique which uses successive orthogonal directions, but these successive directions do not necessarily form a mutually orthogonal set.

The basic elements of the Rosenbrock algorithm are as follows:

a) Step size - The step size in a given direction is chosen by specifying an arbitrary magnitude e and then, if a step e decreases the value of the function (for a minimization problem), e is multiplied by a constant α ($\alpha > 1$). If the value of the function increases, e is multiplied by a constant $-\beta$ ($0 < \beta < 1$). e, α, and β have to be specified by the user. e should be on the order of one percent of the average magnitude of the variables. To determine the values of α and β, a series of trials using various values of α and β should be made for a given class of functions (preferably for a known function for which a solution is available) for which the function to be minimized belongs.

b) Direction - The Rosenbrock algorithm uses N orthogonal directions $d_1, d_2, \ldots, d_N$ at each stage rather than choosing a single direction in which to progress. A search is made in each orthogonal direction before continuing to the next stage (at least, one trial has been successful (a value less than or equal to the old value) and one has failed in each direction).

There are three cases to consider:

i) The first trial is a success.

ii) The first trial is a failure and the second trial is a success.

iii) The first trial is a failure and the second trial is a failure.

For a start, let $[D^0] = [I]$ (identity matrix) where $d_1^0, d_2^0, \ldots d_N^0$ are individual directions in which steps are to be taken. The search technique progresses as follows (for one variable x_i):

1) A step is taken in the direction d^0 from an initial point x^0

$$x^1 = e(x^0 \cdot d^0) .$$

2) If $f(x^1) < f(x^0)$, the step is successful (case (i)) and the step size is multiplied by α again and again until a failure is recorded. After this failure, the result of the last successful trial and the number of successful trials is stored.

3) If $f(x^1) > f(x^0)$ on the first trial (a failure - case (ii)), the sign of the step size e is changed and the search continues as in (2).

4) If $f(x^1) > f(x^0)$ and $f(x^2) > f(x^0)$, the second and further trials are determined by multiplying e by minus β until a success is recorded.

After a search has been made for each variable in all directions d_i^0, a new $[D^1]$ is determined using the Gram-Schmidt orthogonalization procedure. The orthogonalization procedure completes the first search cycle and the same procedure is repeated in the new direction $[D^1]$. The procedure is continued until a convergence criterion is satisfied.

2) Description

The subroutine ROSIEM (N,N1,N2,AA,BB,STEP,CUL,EF,ERR,GOM, PAT,V,XLOAD,ZA) determines the loads $\{X_L^i\}$ and excitation voltage V^a which minimize the pattern synthesis error ε (equation 24).

The input variables are defined as follows:

N = number of antenna elements

N1 = number of search cycle (if N1 = 1, [D] = [I])

N2 = p (number of pattern points)

AA = α

BB = β

STEP = step size e

CUL = $[Z_A + Z_L]^{-1}\vec{V}$

EF = $F(\phi_p)$

ERR = ε(equation 24)

GOM = $|f_o(\phi_p)|$

PAT = $e^{jk(x_n\cos\phi_p+y_n\sin\phi_p)}$

V = V^a (excitation voltage)

XLOAD = $\{X_L^i\}$

ZA = port impedance matrix Z_A(equation 12).

Minimum allocations are given by

```
COMPLEX     CUL(N), EF(N2), PAT(N,N2) ZA(N*N)
DIMENSION   A(N*N), D(N), GOM(N2), NS(N), U(N*N),XL(N),XLOAD(N)
```

Subroutine ERROR is called by subroutine ROSIEM to determine a new value for ε for given $\{X_L^i\}$ and V^a. ROSIEM searches in N variables (N-1 reactive loads (the driven element is not reactively loaded) and one excitation voltage).

The statement "IF (N1-1) 10, 10, 11" sets [D] = [I] and determines $f(X^0)$ if N1 = 1.

DO loop 14 is the main search loop for the N variables. Nested DO loop 20 performs two functions. The first is to increment X_L^i and the second is to determine if the magnitude of the current load value has exceeded 500 ohms. Once the load value has reached 500 ohms, it has been found that further increases in this load value toward infinity will not noticeably change the value of $|F(\phi)|$. Therefore, DO loop 20 will determine when a load magnitude has exceeded 500 ohms and sets the load magnitude equal to A1 ohms and a sign corresponding to the negative of the former reactance. For instance, if X_L^2 = -550 ohms, X_L^2 becomes + A1 ohms. In addition, DO loop 20 resets the value of E (current magnitude of e) to that of STEP and resets N1 to 1 since d_2^{N1} will be incorrect for the new load value. Therefore everytime a load value goes through infinity, $[D^{N1}] = [D^0] = [I]$.

Nested statement "GO TO (21,22,23,24),L" corresponds to the success and failure increment logic for each search cycle. The following is a summary of the logic:

a) Statement 21 is the initial screening logic. If $f(X^1) < f(X^0)$ (the first step is a success), $e^{new} = \alpha e^{old}$ and statement 23 takes over for subsequent steps. If $f(X^1) > f(X^0)$ (the first step is a failure), $e^{new} = -\beta e^{old}$ and statement 22 takes over for the next step.

b) Statement 22 is used if the first step was a failure. If $f(X^2) < f(X^1)$ (the first step was a failure but the second step was a success), $e^{new} = \alpha e^{old}$ and statement 23 takes over for subsequent steps. If $f(X^2) > f(X^1)$ (first two steps were failures), $e^{new} = -\beta e^{old}$ and statement 24 takes over for subsequent steps.

c) Statement 23 is used if the first step was successful or if the first step was a failure and the second step was successful. If $f(X^i) < f(X^{i-1})$, $e^{new} = \alpha e^{old}$. If $f(X^i) > f(X^{i-1})$, $e^{new} = e^{old}/\alpha$ and the search is ended for this variable for the present search cycle. In other words, statement 23 continues to take steps as long as they are successful until the first failure is recorded.

d) Statement 24 is used if the first two steps are failures. If $f(X^i) < f(X^0)$, the search is ended for this variable. If $f(X^i) > f(X^0)$ (continuing failures), $e^{new} = -\beta e^{old}$ (a maximum of 20 $(-\beta)$ steps can be taken before the search ends in this variable).

The variable NS(M) records the number of steps taken for variable number M. If NS(M) is positive, NS(M) will indicate the number of steps taken in the successful direction. If NS(M) is negative, NS(M) will indicate the number of steps taken in the failure direction. If NS(M) equals -20, statement 31 will discontinue the search in this variable until a new direction vector d_i is determined.

The variable D(M) is the final step magnitude for the current search cycle.

DO loops 40 and 42 are the main loops for finding [D^{new}] by the Gram-Schmidt orthogonalization procedure.

3) Listing of Subroutine ROSIEM.

```
      SUBROUTINE ROSIEM(N,N1,N2,AA,BB,STEP,CUL,EF,ERR,GOM,PAT,V,XLOAD,ZA
     1)
      COMPLEX CUL(7),EF(36),PAT(7,36),ZA(49)
      DIMENSION A(49),D(7),GOM(36),NS(7),U(49),XL(7),XLOAD(7)
      N3=N-1
      A1=300.
      IF(N1-1) 10,10,11
   10 J1=0
      DO 12 J=1,N
      J2=J1+J
      DO 13 I=1,N
      J1=J1+1
   13 U(J1)=0.
   12 U(J2)=1.
      CALL ERROR(N,N2,EF,ERR,GOM,PAT,V,XLOAD,ZA)
   11 DO 14 M=1,N
      NS(M)=0
      L=1
      E=STEP
      ERR1=ERR
   15 J1=M
      K=2
      DO 20 I=1,N3
      XL(K)=XLOAD(K)+E*U(J1)
      IF(ABS(XL(K)).GT.501.) N1=0
      IF(ABS(XL(K)).GT.501.) E=SIGN(STEP,XL(K))
      IF(ABS(XL(K)).GT.501.) XLOAD(K)=-SIGN(A1,XL(K))
      IF(ABS(XL(K)).GT.501.) XL(K)=-SIGN(A1,XL(K))
      K=K+1
   20 J1=J1+N
      XL(1)=0.
      V=V+E*U(J1)
      ERR2=ERR
      CALL ERROR(N,N2,EF,ERR,GOM,PAT,V,XL,ZA)
      DERR=ERR-ERR2
      GO TO (21,22,23,24),L
   21 L=3
      IF(DERR) 25,25,26
   26 L=2
      ERR=ERR2
      E=-STEP
      GO TO 15
   22 L=3
      IF(DERR) 25,25,30
   30 L=4
   31 IF(NS(M)+20) 32,32,33
   33 E=-BB*E
      NS(M)=NS(M)-1
      GO TO 15
   25 E=AA*E
      NS(M)=NS(M)+1
      GO TO 15
   23 IF(DERR) 25,25,34
   34 E=E/AA
      ERR=ERR2
      GO TO 32
   24 DERR=ERR1-ERR
      IF(DERR) 31,31,32
   32 J1=M
      K=2
```

```
      DO 35 I=1,N3
      XLOAD(K)=XLOAD(K)+E*U(J1)
      K=K+1
   35 J1=J1+N
      V=V+E*U(J1)
   14 D(M)=E
      J1=N*N+1
      DO 40 I=1,N
      J1=J1-1
      A(J1)=D(N)*U(J1)
      GO TO (40),N
      J3=N
      DO 41 M=2,N
      J2=J1
      J1=J1-1
      J3=J3-1
   41 A(J1)=A(J2)+D(J3)*U(J1)
   40 CONTINUE
      DO 42 M=1,N
      J1=M
      DO 43 I=1,N3
      XL(I)=A(J1)
   43 J1=J1+N
      V=A(J1)
      GO TO (44),M
      MM=M-1
      DO 45 J=1,MM
      Z1=0.
      J1=J
      J2=M
      DO 50 K=1,N
      Z1=Z1+A(J2)*U(J1)
      J1=J1+N
   50 J2=J2+N
      J1=J
      K=2
      DO 51 I=1,N3
      XL(K)=XL(K)-Z1*U(J1)
      K=K+1
   51 J1=J1+N
      V=V-Z1*U(J1)
   45 CONTINUE
   44 C=0.
      K=2
      DO 52 I=1,N3
      C=C+XL(K)*XL(K)
   52 K=K+1
      C=C+V*V
      C=1./SQRT(C)
      J1=M
      K=2
      DO 53 I=1,N3
      U(J1)=C*XL(K)
      K=K+1
   53 J1=J1+N
      U(J1)=C*V
   42 CONTINUE
      RETURN
      END
```

Jan 1974

DISTRIBUTION LIST FOR ONR ELECTRONICS PROGRAM OFFICE

Director
Advanced Research Projects Agency
Attn: Technical Library
1400 Wilson Boulevard
Arlington, Virginia 22209

Office of Naval Research
Electronics Program Office (Code 427)
800 North Quincy Street
Arlington, Virginia 22217

Office of Naval Research
Code 105
800 North Quincy Street
Arlington, Virginia 22217

Naval Research Laboratory
Department of the Navy
Attn: Code 2627
Washington, D. C. 20375

Office of the Director of Defense
Research and Engineering
Information Office Library Branch
The Pentagon
Washington, D. C. 20301

U. S. Army Research Office
Box CM, Duke Station
Durham, North Carolina 27706

Defense Documentation Center
Cameron Station
Alexandria, Virginia 22314

Director National Bureau of Standards
Attn: Technical Library
Washington, D. C. 20234

Commanding Officer
Office of Naval Research Branch Office
536 South Clark Street
Chicago, Illinois 60605

San Francisco Area Office
Office of Naval Research
50 Fell Street
San Francisco, California 94102

Air Force Office of Scientific Research
Department of the Air Force
Washington, D. C. 20333

Commanding Officer
Office of Naval Research Branch Office
1030 East Green Street
Pasadena, California 91101

Commanding Officer
Office of Naval Research Branch Office
495 Summer Street
Boston, Massachusetts 02210

Director
U. S. Army Engineering Research
and Development Laboratories
Fort Belvoir, Virginia 22060
Attn: Technical Documents Center

ODDR&E Advisory Group on Electron Devices
201 Varick Street
New York, New York 10014

New York Area Office
Office of Naval Research
207 West 24th Street
New York, New York 10011

Air Force Weapons Laboratory
Technical Library
Kirtland Air Force Base
Albuquerque, New Mexico 87117

Air Force Avionics Laboratory
Air Force Systems Command
Technical Library
Wright-Patterson Air Force Base
Dayton, Ohio 45433

Air Force Cambridge Research Laboratory
L. G. Hanscom Field
Technical Library
Cambridge, Massachusetts 02138

Harry Diamond Laboratories
Technical Library
Connecticut Avenue at Van Ness, N. W.
Washington, D. C. 20438

Naval Air Development Center
Attn: Technical Library
Johnsville
Warminster, Pennsylvania 18974

Naval Weapons Center
Technical Library (Code 753)
China Lake, California 93555

Naval Training Device Center
Technical Library
Orlando, Florida 22813

Naval Research Laboratory
Underwater Sound Reference Division
Technical Library
P. O. Box 8337
Orlando, Florida 32806

Navy Underwater Sound Laboratory
Technical Library
Fort Trumbull
New London, Connecticut 06320

Commandant, Marine Corps
Scientific Advisor (Code AX)
Washington, D. C. 20380

Naval Ordnance Station
Technical Library
Indian Head, Maryland 20640

Naval Ship Engineering Center
Philadelphia Division
Technical Library
Philadelphia, Pennsylvania 19112

Naval Postgraduate School
Technical Library (Code 0212)
Monterey, California 93940

Naval Missile Center
Technical Library (Code 5632.2)
Point Mugu, California 93010

Naval Ordnance Station
Technical Library
Louisville, Kentucky 40214

Naval Oceanographic Office
Technical Library (Code 1640)
Suitland, Maryland 20390

Naval Explosive Ordnance Disposal Facility
Technical Library
Indian Head, Maryland 20640

Naval Electronics Laboratory Center
Technical Library
San Diego, California 92152

Naval Undersea Warfare Center
Technical Library
3202 East Foothill Boulevard
Pasadena, California 91107

Naval Weapons Laboratory
Technical Library
Dahlgren, Virginia 22448

Naval Ship Research and Development Center
Central Library (Code L42 and L43)
Washington, D. C. 20007

Naval Ordnance Laboratory White Oak
Technical Library
Silver Spring, Maryland 20910

Naval Avionics Facility
Technical Library
Indianapolis, Indiana 46218